Highly sensitive type IA fiber Bragg gratings as sensors in radiation environments

A.Faustov [1,3], P. Saffari [2], C. Koutsides [2,4], A. Gusarov [1], M. Wuilpart [3], P. Mégret [3], L. Zhang [2], K. Kalli [4] [*]

[1] SCK•CEN Belgian Nuclear Research Center, Boeretang 200, 2400 Mol, Belgium
[2] Aston University, Birmingham, B4 7ET, United Kingdom
[3] University of Mons, Boulevard Dolez 31, 7000 Mons, Belgium
[4] Cyprus University of Technology, 33 Saripolou Street, Limassol, 3036, Cyprus

ABSTRACT

Type IA fiber gratings have unusual physical properties compared with other grating types. We compare with performance characteristics of Type IA and Type I Bragg gratings exposed to the effects of Co[60] gamma-irradiation. A Bragg peak shift of 190 pm was observed for Type IA gratings written in Fibercore PS-1250/1500 photosensitive fiber at a radiation dose of 116 kGy. This is the largest wavelength shift recorded to date under radiation exposure. The Type IA and Type I gratings show different kinetics under radiation and during post-radiation annealing; this can be exploited for the design of a grating based dosimetry system.

Keywords: Fiber Bragg gratings, ionizing radiation effects, fiber optic dosimetry

1. INTRODUCTION

It has been well documented that fiber Bragg gratings (FBGs) are sensitive to ionizing radiation [1, 2]. The actual wavelength shift on exposure to the ionizing radiation is principally dependent on the fiber type and conditions of any fiber processing, such as photosensitization. For example, an ionizing radiation-induced dose of tens of kGy leads to a Bragg wavelength shift (BWS) of several tens of pm for gratings written in intrinsically photosensitive Ge-doped fibers and this increases further for gratings written in hydrogen loaded fiber. This is interesting for sensing, however, any radiation-induced BWS will compromise the performance of FBG-based telecommunication devices and sensors, operating in near-earth space radiation environments [3]. Clearly, as the BWS increases with radiation dose, we can exploit the radiation sensitivity of FBGs to design a dosimeter with a number of important advantages, such as small dimensions, light weight, possibility for on-line dose monitoring. In particular, these are considered critical for the application of space instrumentation. The mechanism of the radiation sensitivity of FBGs is generally well understood, being attributed to the generation of radiation defects, and depends on the fiber and fabrication parameters [4, 5]. However, one cannot make any quantitative prediction of the BWS for a particular grating and radiation testing remains the only viable method for grating validation. Irradiation testing of gratings written in a variety of fibers under a diverse range of conditions has shown gratings with ~160 pm BWS at a 100 kGy dose [5]. This is a substantial shift but even higher values are desirable as demonstrated in this work, where we direct our attention to new FBG developments.

The Type IA gratings [6], are rapidly inscribed in suitably prepared hydrogen-loaded fibers [7]. The Type IA is essentially a subtype of Type I gratings, and this grating type is indistinguishable from a Type I in a static situation. Their inscription characteristics however are quite different, with a large increase in the mean core index, identifiable as a large red shift in the grating Bragg wavelength λ_B. λ_B is dependent on fiber type and hydrogenation conditions, but it saturates, for a highly doped fiber (either high Ge dopant or B/Ge co-doped fiber) at 15 to 20 nm, and 5 to 8 nm for SMF-28 fiber. The maximum wavelength shift translates to an increase in the mean index of up to 2×10^{-2}.

*kkalli@cytanet.com.cy, kyriacos.kalli@cut.ac.cy; phone 35725002609; www.cut.ac.cy

Furthermore, Type IA gratings exhibit the lowest temperature coefficient of all grating types reported to date, making them ideal for use in a temperature compensating, dual grating sensor [8]. It is interesting to assess the radiation sensitivity of Type IA gratings for dosimetry purposes. Firstly, hydrogen loading is a relevant condition for a significant BWS. Secondly, Type IA gratings have lower temperature stability compared to standard gratings, which can be considered as an indication of higher structural damage due to the grating inscription with prolonged UV-exposure. A damaged atomic structure should be more sensitive to ionizing radiation as compared to the structure of Type I gratings.

1.1 FBG fabrication and properties

A series of Type I and IA FBG pairs were inscribed in the same optical fiber length. Three different fiber types were used: Fibercore PS-1250/1500, a B/Ge co-doped fiber; Fibercore SM-1500, a high-Ge-doped fiber, and a B/Ge co-doped fiber. All fibers were hydrogenated at 200 bar and 80°C for 48 hours and stored at -40°C before FBG inscription, using a method similar to the standard phase mask technique. The phase mask length, width and period were 50 mm, 3.0 mm and 1060.85 nm, respectively. In order to inscribe a Type IA grating in the PS 1250/1500 fiber, a 5 mm fiber length was pre-exposed to UV radiation from a Sabre FreD laser (244 nm emission wavelength) with a 200 mW power. The fiber section was scanned more than 20 times with a scan velocity of 0.05 mm/s, with the phase mask removed. The transmission spectrum was monitored using a broadband light source and an optical spectrum analyzer. During this blank beam exposure process an absorption band at 1400 nm related to the formation of OH bonds in the fiber induced a transmission loss of 14 dB. This feature does not depend on the modulated index change needed for FBG fabrication, but gives accurate feedback regarding the fiber maturity required for Type IA inscription. The phase mask was reintroduced and a Type IA grating was formed by UV scanning a 3-mm length of the pre-exposed area with a scan velocity 0.01 mm/s. We finally inscribed a 5-mm long standard FBG located 3 mm from the pre-exposed region of the fiber by employing the same phase mask setup. The Type IA grating appears on the longer wavelength side of the Type I FBG, red-shifted by 16.8 nm. A ghost mode (a weak dip at 1538 nm in Fig. 2) often appears; due to the increase in the mean core refractive index. This method was used for Type I-IA FBG inscription in the SM1500 and B/Ge co-doped fibers.
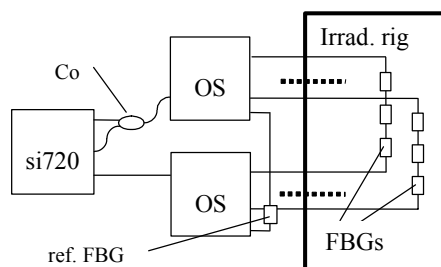

Fig. 1. Experimental set-up. OS – optical switch; Co – 50x50 coupler; si720 – Micron Optics Optical

The characterization set-up (Fig. 1) relies on a FBG interrogation system si720 from Micron Optics (wavelength range: 1520 to 1570 nm). Two single-mode (E-Tek) optical switches allow for sequential FBG measurements in transmission and reflection. The set-up included a temperature-stabilized FBG to monitor the long-term stability. The set-up wavelength stability throughout the experiment is within ±1.5 pm, with 24h variations below ±1 pm.

2. RESULTS AND DISCUSSION

Final measurements were made at the underwater irradiation facility RITA (Radio Isotope Test Arrangement) at SCK-CEN. The RITA facility has 4 cylindrical Co^{60} sources located 6 m below the water surface, where a water tight container is placed in the middle of the square formed by these sources. The non-uniformity of the dose-rate distribution over the FBGs was less than 5%. Fig. 2 shows the transmission spectra for the chain #5, as summarized in Table 1 and the BWS during the experiment. A monotonous BWS is observed for all the gratings, with a record value above 190 pm at the end of irradiation for the Type IA grating written in the PS-1250 fiber when 116 kGy ionizing radiation dose was accumulated (Fig. 2).

Table 1. FBG characteristics at 0°C

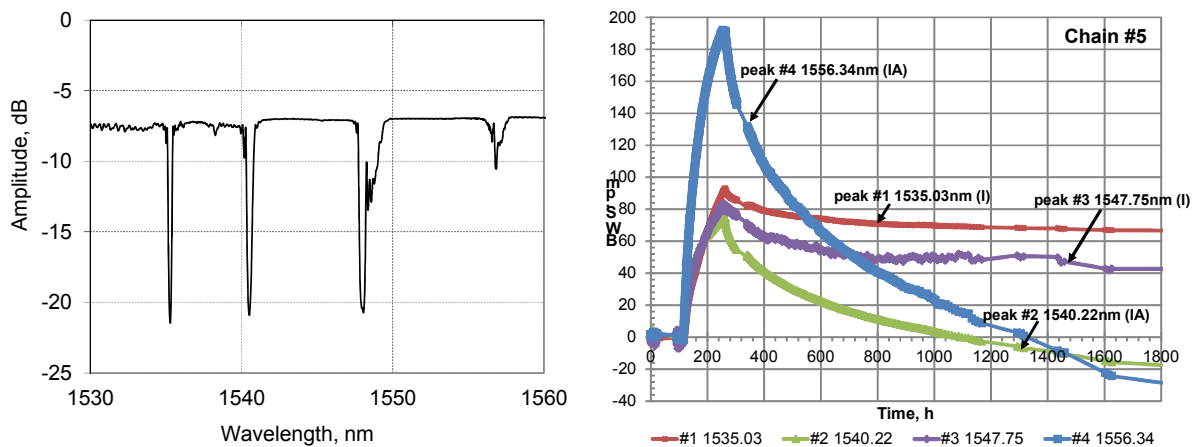|	Fiber	peak #1 nm/dB(Type)	peak #2 nm/dB(Type)	peak #3 nm/dB(Type)	peak #4 nm/dB(Type)
#5	PS 1250, SM 1500	1535.0/14.2(I)	1540.2/13.4 (IA)	1547.8/10.8(I)	1556.3/3.4 (IA)
#6	B/Ge	1534.4/5.2 (I)	1545.6/23.6 (IA)		
#7	B/Ge	1533.8/3.9(I)	1540.3/4.4(I)	1545.5/7.5(IA)	
#8	B/Ge, SM 1500	1535.1/12.7 (I)	1545.9/36.0 (IA)	1549.2/49.7 (I)	1557.4/13.7 (IA)
#9	PS 1250	1533.3/7.6(I)	1547.7/4.0(IA)		

Fig. 2. Transmission spectrum before irradiation (left) and the BWS (right) for the gratings in Chain #5. The gratings with the Bragg wavelength at 1535.0 and 1547.8 nm are of Type I and at 1540.2 and 1556.3 nm - Type IA.

The BWS shows a saturating tendency under radiation that results in the dose sensitivity decrease when irradiation dose increases. For instance, for the FBG in the chain #5 peaking at 1535.0 nm (see Fig. 3) the minimal detectable dose increment, which stems from the measurement resolution of ±1 pm, changed from 130 Gy at the beginning of the irradiation to 300 Gy at the end. The FBGs with the Bragg peaks at 1540.2 and 1556.3 nm had fairly close values, while for the third one (1547.8 nm) the initial minimal sensitivity was already 470 Gy. Also the third FBG had a very high dispersion of data that was probably due to a lower quality of the FBG. On the other hand, the saturation level was not reached and even larger BWSs could be obtained with the radiation dose suitably increased.
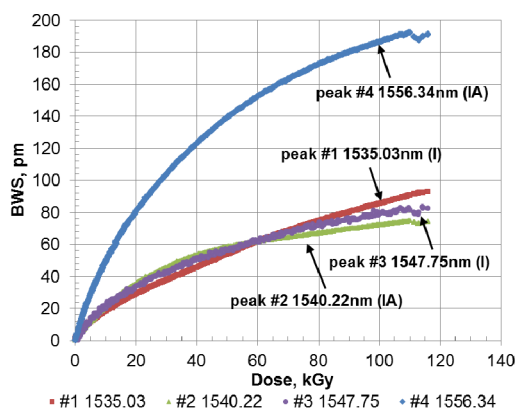

Fig. 3. Kinetics of the BWS during irradiation as a function of the accumulated dose for the chain #5.

Post-irradiation annealing is a well-known effect for FBGs and usually for the radiation-induced BWS the shift recovery is well below 50% of the maximal value. However, for the Type IA gratings the annealing is so strong that a negative (short-wavelength) BWS is observed for >1000 h after the irradiation. We interpret this as an indication that two types of defects are generated under ionizing radiation [9]. One defect type is responsible for the long-wavelength shift, while the other accounts for the effective refractive index decrease. Under irradiation the growth of the first type defects' concentration is faster and the net effect corresponds to the long wavelength shift. However, these defects are less stable compared to the defects of the second group, and as a result of their faster annealing the BWS changes from the long-wavelength to the short wavelength one.

Our goal has been to identify highly sensitive FBGs suitable for dosimetry applications. The observed BWS is nonlinear with respect to the dose as a result of saturation and annealing. Therefore, to reconstruct the dose continuous BWS monitoring is required. The temperature has also to be measured because of the annealing speed's temperature dependence. It is therefore very important to find the mechanisms responsible for the negative BWS because its control would allow temperature and radiation effects differentiation. This work is now in progress. Irradiated Type I gratings also demonstrate a significant BWS up to 85 pm for the grating written in the PS 1250 fiber, with a limited post-irradiation BWS recovery. This response compares well to existing results. It seems likely that different kinetics under radiation and during post-radiation annealing together with significantly different temperature sensitivity of Type IA and Type I gratings should allow discrimination of temperature and radiation induced effects.

3. CONCLUSION

We have studied Co^{60} gamma-radiation effect on the Bragg wavelength and the amplitude of Type IA and Type I FBGs. A record Bragg peak shift of 190 pm was observed in Type IA grating at a radiation dose of 116 kGy. We believe that even higher Bragg peak shifts are possible provided we find a way to reduce the radiation defects responsible for the short-wavelength BWS. The Type IA gratings show post-irradiation annealing kinetics that differ markedly from Type I and Type IIA gratings. We consider that two types of radiation defects are created. Defects of one type are responsible for long-wavelength Bragg shift, whereas the generation of another defect type results in the short wavelength shift.

REFERENCES

[1]   A. Othonos, and K. Kalli, *Fiber Bragg Gratings, Fundamentals and Applications in Telecommunications and Sensing*: Artech House, 1999.

[2]   F. Berghmans, and A. Gusarov, "Fiber Bragg grating sensors in space and nuclear environments," *Fiber Bragg Gratings Sensors: Thirty Years from Research to Market*, A. Cusano, A. Cutolo and J. Albert, eds.: Bentham, 2011.

[3]   A. I. Gusarov, D. B. Doyle, N. Karafolas, and F. Berghmans, "Fiber-Bragg-Gratings as a candidate technology for satellite optical communication payloads: radiation - induced spectral effects," Photonics for Space and Enhanced Radiation environments VII, San Diego, CA, E. Taylor, ed., Proc. SPIE, v. 4134, pp. 253-260.

[4]   H. Henschel, S. K. Hoeffgen, K. Krebber, J. Kuhnhenn, and U. Weinand, "Influence of fiber composition and grating fabrication on the radiation sensitivity of fiber Bragg gratings," *IEEE Trans. Nuclear Sci.,* vol. 55, no. 4, pp. 2235-2242, Aug, 2008.

[5]   H. Henschel, S. K. Hoeffgen, J. Kuhnhenn, and U. Weinand, "Influence of manufacturing parameters and temperature on the radiation sensitivity of fiber Bragg gratings," *IEEE Trans. Nuclear Sci.,* vol. 57, 2010.

[6]   A. G. Simpson, K. Kalli, K. Zhou, L. Zhang, and I. Bennion, "Formation of type IA fibre Bragg gratings in germanosilicate optical fibre," *Electron. Lett.,* vol. 40, no. 3, pp. 127-33, 2004.

[7]   A. G. Simpson, K. Kalli, K. Zhou, L. Zhang, and I. Bennion, "Blank beam fabrication of regenerated type IA gratings," *Meas. Sci. Technol.,* vol. 15, pp. 1665-9, 2004.

[8]   A.G. Simpson, K. Kalli, K. Zhou, L. Zhang, I. Bennion, An idealised method for the fabrication of temperature invariant IA-I strain sensors, K. Hotate (Ed.) OFS-16, The Institute of Electronics, Information and Communication Engineers, Nara, Japan, 2003, pp. PD4.

[9]   A. Gusarov, D. Kinet, C. Caucheteur, M. Wuilpart, and P.Mégret, "Gamma radiation induced short-wavelength shift of the Bragg peak in Type I fiber gratings," *IEEE Trans.Nucl.Sci.,* vol. 57, no. 6, pp. 3775-8, 2010.